# Differential stabilization of reaction intermediates: specificity checkpoints for M.EcoRI revealed by transient fluorescence and fluorescence lifetime studies

Ben Youngblood[1], Eleanor Bonnist[2,3], David T. F. Dryden[2,3], Anita C. Jones[2,3] and Norbert O. Reich[1,4,*]

[1]Program in Biomolecular Science and Engineering, University of California, Santa Barbara, CA 93106-9510, USA, [2]School of Chemistry, [3]Collaborative Optical Spectroscopy, Micromanipulation and Imaging Centre (COSMIC), The University of Edinburgh, West Mains Road, Edinburgh EH9 3JZ, UK and [4]The Department of Chemistry and Biochemistry, University of California, Santa Barbara, CA 93106-9510, USA

## ABSTRACT

**M.EcoRI, a bacterial sequence-specific *S*-adenosyl-ʟ-methionine-dependent DNA methyltransferase, relies on a complex conformational mechanism to achieve its remarkable specificity, including DNA bending, base flipping and intercalation into the DNA. Using transient fluorescence and fluorescence lifetime studies with cognate and noncognate DNA, we have characterized several reaction intermediates involving the WT enzyme. Similar studies with a bending-impaired, enhanced-specificity M.EcoRI mutant show minimal differences with the cognate DNA, but significant differences with noncognate DNA. These results provide a plausible explanation of the way in which destabilization of reaction intermediates can lead to changes in substrate specificity.**

## INTRODUCTION

*S*-adenosyl-ʟ-methionine-dependent bacterial DNA methyltransferases modify bases at cytosine (C5 and N4), and adenine (N6), and play important roles in many cellular pathways including mismatch repair, restriction modification and gene regulation (1). Some of these enzymes are viable candidates for antibiotic and cancer drug development respectively (2–5). DNA methyltransferases have a complex reaction mechanism involving several conformational changes in order to position the target base extrahelical so that methyl-transfer may occur.

Base flipping was originally observed in the ternary crystal structure of the cytosine methyltransferase M.HhaI (6). Subsequent structures of other ternary methyltransferase complexes revealed an extrahelically poised target base in the active site of the enzyme (7). Base flipping appears to be important for all DNA methyltransferases as well as other classes of nucleic acid-modifying enzymes.

The bacterial DNA adenine methyltransferase EcoRI forms part of a restriction/modification system and modifies the N6 position of the second adenine in the sequence GAATTC. The transient nature of the core methyltransferase intermediate, in which the target base is extrahelical, was measured first with M.EcoRI using the fluorescent base analog 2-aminopurine (2AP) (8). Analysis of 2AP fluorescence by monitoring the decay of the signal (lifetime analysis) provides new insights into the nature and population of conformational intermediates. 2AP lifetime analysis was previously carried out with the cytosine methyltransferase M.HhaI in complex with a DNA (9). These solution-based studies revealed four distinct populated environments of the target base which were also apparent in the fluorescence decays of the crystalline enzyme–cofactor–DNA complexes (9). Crystallographically resolvable intermediates with the adenine methyltransferase M.TaqI were recently assigned using solution and crystalline 2AP lifetime analysis (10).

Our previous efforts to understand M.EcoRI's discrimination mechanism (11,12) were in part motivated by our work with a bending-impaired M.EcoRI mutant (H235N) whose ability to flip its target adenine is decreased 2000-fold compared to the WT enzyme, while the activity was left largely intact (13). Moreover, the mutant is at least 1000-fold more discriminating than the

WT enzyme for recognition of the cognate target (12,13). The molecular basis of how changes in precatalytic conformational transitions, as observed with DNA polymerases (14,15), can result in such a profound increase in specificity is the focus of this study. The M.EcoRI-mediated conformational changes including DNA bending, intercalation and base flipping have been studied in detail for M.EcoRI. Here we extend these studies to include fluorescence decay to provide insight into how both the wild-type and mutant enzymes discriminate between cognate and noncognate DNA.

## MATERIALS AND METHODS

### Enzyme expression and purification

M.EcoRI was purified from MM294 *Escherichia coli* cells with the plasmid pXRI as previously described (16). Six liters of culture were induced with 1mM IPTG at an $OD_{600}$ nm 0.4 for 3 h. Cells were sonicated in extraction buffer [200 mM NaCl, 6.5 mM $K_2HPO_4$, 3.5 mM $KH_2PO_4$, 1 mM EDTA and protease inhibitor mixture (Sigma)]. The lysate was centrifuged (30 min at 4°C), the supernatant was loaded onto a 20-ml phosphocellulose (Whatman) column and the protein was eluted with a salt gradient between 200 and 800 mM NaCl. Fractions containing M.EcoRI were loaded onto a 10 ml hydroxyapatite (Bio-Rad) column equilibrated with extraction buffer. The protein was eluted with a gradient between 6.5 mM and 1 M $KH_2PO_4$, and dialyzed overnight in extraction buffer containing 10% glycerol. The dialyzed protein was loaded onto a biorex (Bio-Rad) column, and the protein was eluted with a gradient of 200 mM and 800 mM NaCl. Protein from this procedure was typically >95% pure by densitometry. Enzymes were stored at –80°C with 10% (v/v) glycerol, 0.3–0.4 M NaCl, 10 mM potassium phosphate (pH 7.8), 1 mM EDTA and 7.5 mM β-mercaptoethanol.

### DNA synthesis and fluorophore coupling

Fluorescently labeled oligonucleotides were prepared as previously described (16). DNA oligonucleotides for fluorophore coupling were synthesized at Integrated DNA Technologies containing 5′ C-6 primary amino modifications. 2AP containing oligonucleotides were purchased at Midlands DNA with the target adenine replaced by the 2AP nucleotide. Fourteen mer top strands cognate 5′-AGACGAATTCCGAA and noncognate (A4) 5′-AGACGAATTTCGAA; Fourteen mer bottom strands cognate 5′-TTCGGAATTCGTCT and noncognate (A4) 5′-TTCGAAATTCGTCT. All bottom-strand target adenines were methylated to force the orientation of the enzyme to target the top strand. Oligonucleotides for fluorescence resonance energy transfer (FRET) studies were coupled as previously described (16). Briefly, oligonucleotides were resuspended in $dH_2O$, extracted with chloroform, ethanol precipitated and resuspended to a final concentration of 25 μg/μl. 6-Alexa Fluor 488 succinimidyl ester (Molecular Probes) was coupled to the top strand, while 6-carboxytetramethylrhodamine succinimidyl ester (Molecular Probes) was coupled to the

bottom strand. Coupling reactions were performed with 10–20-fold molar excess dye to oligonucleotide. Coupling was carried out overnight in 75 mM sodium tetraborate (pH 8.5). Overnight couplings were ethanol precipitated and resuspended in 0.1 M triethylammonium acetate. Resuspended coupling reactions were purified on an analytical Vydac C4 column with a Waters/Millipore HPLC system. Purified coupled oligonucleotide concentrations were determined by absorbance scans from 230 to −700 nm and determined to be 100% coupled.

### Equilibrium FRET

Equilibrium fluorescence experiments were performed as previously described (12,16). All measurements were collected with a Perkin Elmer LS50B luminescence spectrometer at 22°C. Excitation at 485 nm was used to excite Alexa-488, and an emission spectrum from 500 to 650 nm was collected. Enzyme at a final concentration of 200 nM was mixed with 20 nM DNA and 1 μM sinefungin in reaction buffer (50 mM Tris, pH 8.0, 5 mM EDTA, 100 mM NaCl and 1 mM DTT). The AdoMet analog sinefungin (Sigma–Aldrich) was used for all equilibrium and transient experiments.

### Stopped flow FRET

Stopped flow measurements were collected on an Applied Photophysics SX.18MV stopped flow reaction analyzer outfitted with a single-channel emission photomultiplier tube. An excitation wavelength of 485 nm and an emission cutoff filter of 515 nm were used for data collection. Coupled DNA was rapidly mixed with M.EcoRI preincubated with sinefungin in reaction buffer. The change of donor fluorophore emission was used to detect bending and intercalation due to the greater signal change for the donor fluorophore during FRET with the acceptor fluorophore (12,16). DNA concentrations were 20 nM for cognate DNA and 100 nM for noncognate DNA substrates. Enzyme and cofactor concentrations were varied from 100 to 2000 nM. Error measurements are from at least two experiments with the DNA and enzyme mixes freshly prepared each time.

### Reverse kinetics

2AP fluorescence is roughly 14-fold greater when extrahelical, and has previously been validated as a probe for the measurement of base-flipping kinetics (8,17–19). An excitation wavelength of 310 nm and an emission cutoff filter of 320 nm were used for data collection. The rate of extrahelical base restacking was measured by monitoring the dissociation of the preformed 2AP containing DNA–enzyme complex. The loss of fluorescence is attributed to the restacking of the target base. A final concentration of 100 nM 2AP DNA, 100 nM enzyme and 6 μM Sinefungin were mixed with 5 μM unlabeled competitor DNA. The unbending/unintercalation data were collected by monitoring the change in FRET as a 25–50-fold excess unlabeled cognate DNA was rapidly mixed into the system. Excitation wavelengths and cutoff filters used for unbending/unintercalation are the same described in the 'Stopped flow FRET' section. All forward and reverse
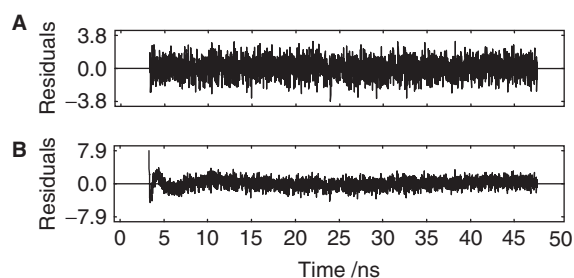
**Figure 1.** Comparison of the residuals obtained for the fit of the experimental decay curve of the A4-WT M.EcoRI-sinefungin complex to (**A**) four lifetime components and (**B**) three lifetime components. The corresponding $\chi^2$ values are (A) 1.03 and (B) 1.3.

stop flow data were fit to either a single or double exponential equation using the program Sigma Plot.

### Fluorescence decay measurement

Fluorescence decay measurements on enzyme–DNA complexes were carried out on samples of the following composition: 2 μM DNA, 6 μM enzyme and 14 μM Sinefungin buffered in 100 mM NaCl, 50 mM Tris, 5 mM EDTA and 1 mM DTT (pH 8).

Fluorescence decays were acquired using the technique of time-correlated single photon counting, following the same general procedure reported previously (9,10). The excitation source was the third harmonic of the pulse-picked output of a Ti-Sapphire femtosecond laser system (Coherent, 10 W Verdi and Mira Ti-Sapphire), consisting of pulses of ∼200 fs at 4.75 MHz repetition rate, at a wavelength of 320 nm. Fluorescence decays were measured in an Edinburgh Instruments spectrometer equipped with TCC900 photon counting electronics. The instrument response of the system was ∼50 ps FWHM. Fluorescence decay curves were analyzed using a standard iterative reconvolution method, assuming a multiexponential decay function. Decays were collected at several emission wavelengths (typically 370, 390 and 410 nm) and analyzed globally using Edinburgh Instruments' FAST software, i.e. they were fitted simultaneously, with lifetimes, $\tau_i$, as common parameters. Fits were made using a multi-exponential decay function, Equation (1)

$$I(t) = \sum_{i=1}^{n} A_i e^{-t/\tau_i} + B \qquad 1$$

where $A_i$ is the fractional amplitude, $\tau_i$ is the fluorescence lifetime of the $i$th decay component, and $B$ is the background level (dark count of the detector).

The value of $A_i$ gives the fractional population of the fluorescent species with lifetime $\tau_i$. The quality of fit was judged on the basis of the reduced chi-square statistic, $\chi^2$, and the randomness of residuals. Typically, we find that a $\chi^2$ value <1.2 indicates an acceptable fit. All of the decay curves measured required four exponential components [a value of $n = 4$ in Equation (1)] to give a satisfactory fit according to these criteria. This is exemplified in Figure 1 which compares the residuals obtained for 4- and 3-component fits to the decay of the the noncognate

duplex bound to WT M.EcoRI. For the 3-component fit (Figure 1B) the residuals are clearly nonrandom and the $\chi^2$ value of 1.3 is unacceptably high. Addition of a fourth decay time results in random residuals (Figure 1A) and a significant reduction in $\chi^2$ to 1.03.

### Steady-state kinetic analysis

As previously described (12,20,21) the constants $K_M^{DNA}$ were measured by titrating in an increasing concentration of DNA into a methylation reaction buffer (100 mM Tris–HCl, pH 8.0, 10 mM EDTA, 10 mM DTT) containing M.EcoRI and $S$-[methyl-$^3$H]adenosyl-L-methionine (Amersham Biosciences). Cognate DNA concentration was varied from 20 to 320 nM. A4 noncognate DNA concentration varied from 0.5 to 32 000 μM. For cognate studies the enzyme and cofactor concentrations used were 5 nM and 6 μM, respectively. Cognate reactions were quenched at 10 min and spotted onto DE81 filter paper. For noncognate studies the enzyme and cofactor concentrations used were 40 nM and 6 μM, respectively. Noncognate reactions were quenched at 60 min and spotted onto DE81 filter paper. Incorporated methyl-$^3$H onto DNA spotted on DE81 filter papers were processed as previously described (22). Values for $K_M^{DNA}$ were obtained by fitting the data to a rectangular hyperbola using the program SigmaPlot.

## RESULTS

Site-specific DNA methylation relies on multiple enzyme-induced conformational intermediates in order to select the correct DNA substrate. DNA bending, intercalation and base flipping involve conformational transitions and reaction intermediates that are differentially populated with cognate and noncognate substrates (12,16). To better understand the importance of each intermediate towards specificity, we used multiple fluorescence techniques to determine both transient and equilibrium DNA bending, intercalation and base-flipping transitions of WT and H235N M.EcoRI.

### Mutation H235N of M.EcoRI decreases the level of DNA intercalation

Prior work revealed that the H235N mutation results in no observable DNA bending as determined by AFM and gel migration experiments (13). Moreover we have previously shown using FRET analysis of DNA bending that WT M.EcoRI induces a ∼50° bend in a cognate substrate, followed by intercalation of residues into the DNA resulting in expansion of the target DNA by increasing the distance between the base-stacked nucleotides (16). These studies were expanded upon using noncognate substrates to examine the role of these conformational changes in substrate selection. It was found that much of M.EcoRI's specificity arises from energetic barriers between the conformational steps of DNA bending, base flipping and intercalation, manifested in slower fluorescent changes when examining FRET of 2AP fluorescence with noncognate substrates (12). To further understand the specificity determinants of M.EcoRI, the transient

**A**



**B**
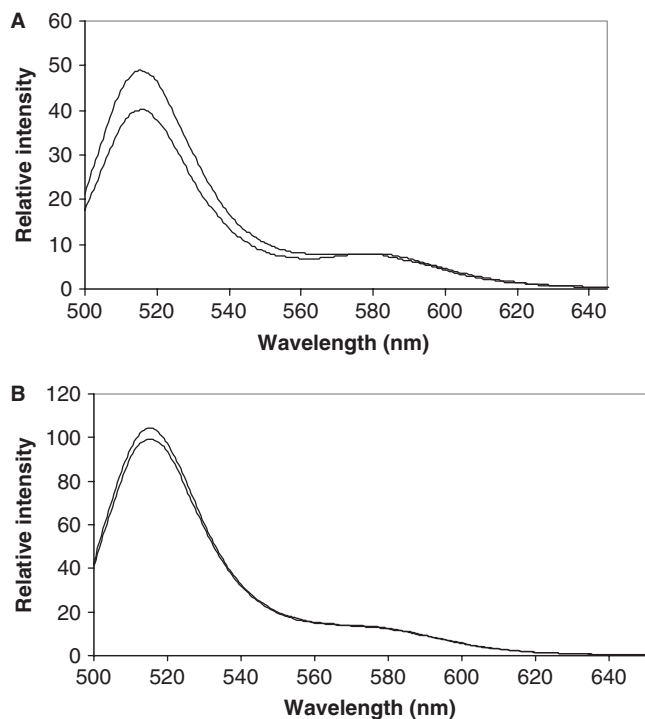


**Figure 2.** Equilibrium FRET of cognate 14mer 5′-Alexa-488/5′-TAMRA DNA. Solid line = DNA alone, dashed line = DNA + M.EcoRI (100 nM) + Sinefungin (6 μM). (**A**) WT M.EcoRI–DNA (10 nM), (**B**) H235N M.EcoRI–DNA (20 nM).

fluorescent techniques which probe DNA bending, base flipping and intercalation were applied to H235N M.EcoRI. Due to the postulated DNA-bending deficiency of H235N M.EcoRI we anticipated that the mutant enzyme would induce a much-reduced equilibrium FRET with the fluorescently labeled cognate DNA. Surprisingly, a small but reproducible increase (4%) in equilibrium FRET is observed with the mutant enzyme versus the decrease (26%) in equilibrium FRET previously observed with the WT enzyme (Figure 2A and B).

To assign the contribution of both DNA bending and intercalation to the newly observed increase in equilibrium FRET the transient kinetics of each step were measured (Figure 3A–C). Bending and intercalation can be measured using FRET with WT enzyme and cognate DNA by monitoring the change in donor emission upon rapidly mixing the enzyme/sinefungin with fluorescently labeled DNA. The rates for forward bending and intercalation of WT and H235N with cognate DNA are concentration dependent (Figure 3A) (12,16), suggesting that the forward rate of bending and intercalation are nearly simultaneous with binding. Differences between the WT and H235N M.EcoRI arise when monitoring the reverse bending and intercalation events. Reverse bending and intercalation rate constants were determined by monitoring the change in the donor emission upon rapidly mixing the enzyme–DNA–sinefungin complex with 50-fold excess unlabeled DNA. The reverse steps for WT M.EcoRI are determined by observing a decrease in the donor signal (Figure 3B). Similar experiments with H235N M.EcoRI

produce an increase in the donor emission fitting to a double exponential equation (Figure 3C) (Table 1). It should be noted that previous characterization of reverse bending/intercalation of WT M.EcoRI with noncognate substrates A4 and A3 also resulted in an increase in donor emission (12). From these observations it was concluded that the WT M.EcoRI–noncognate DNA intercalation intermediate is less populated versus the WT M.EcoRI–cognate DNA complex (12). The change in directionality in the reverse bending/intercalation experiment of H235N M.EcoRI with cognate DNA, similar to WT M.EcoRI with noncognate DNA, suggests that the intercalation intermediate is less populated with the H235N M.EcoRI–cognate DNA complex versus the WT M.EcoRI–cognate DNA complex.

### The H235N mutation changes the local environment of the target base

The reaction intermediate in which the target adenine is positioned extrahelically is poised just prior to methyl-transfer, and thus plays a central mechanistic role. Kinetic fluorescence measurements of the flipped 2AP were employed to quantify the population of this intermediate with both the specificity-enhanced H235N M.EcoRI and WT M.EcoRI. The restacking rate constant for H235N M.EcoRI with cognate DNA is only 4-fold slower than WT M.EcoRI with cognate DNA (Figure 4) (Table 2). As previously described, the transient base-flipping data fit best to a double exponential equation (12,13,23). The two phases of the transient base flipping (13) and restacking data (Figure 4) suggest that at least two base-flipped intermediates exist. The reduction in the rate of base restacking of H235N M.EcoRI (Table 2) further confirms the previous conclusion that the transition state between the flipped and unflipped intermediates is energetically more difficult to achieve with the mutant enzyme (13). Increasing the energetic barrier between base flipped and unflipped most likely arises from a loss in a stabilizing interaction between the target base and the enzyme along the base-flipping trajectory.

In order to more thoroughly examine the differences between WT and H235N M.EcoRI base-flipped intermediates and the transitioning between fully flipped and unflipped intermediates, 2AP fluorescence lifetime decay data (Table 3) were measured with each enzyme bound to cognate DNA. Studying 2AP extrahelical positioning by fluorescence decay measurements reveals a distribution of populated conformations at equilibrium, and the decay parameters describe a superposition of the decays of the various conformations. The unbound cognate duplex shows a 4-exponential fluorescence decay, similar to those observed previously for other 2AP-containing duplexes (9,10). The presence of four different lifetimes indicates that 2AP exists in four distinct molecular environments, signifying the existence of at least four conformational states of the duplex. The fractional amplitude ($A_i$) indicates the fractional population of each conformational state. The two shortest lifetimes, 0.14 and 0.54 ns, account for the vast majority of the population [85% in total $(A_1 + A_2)$] and correspond to well-stacked
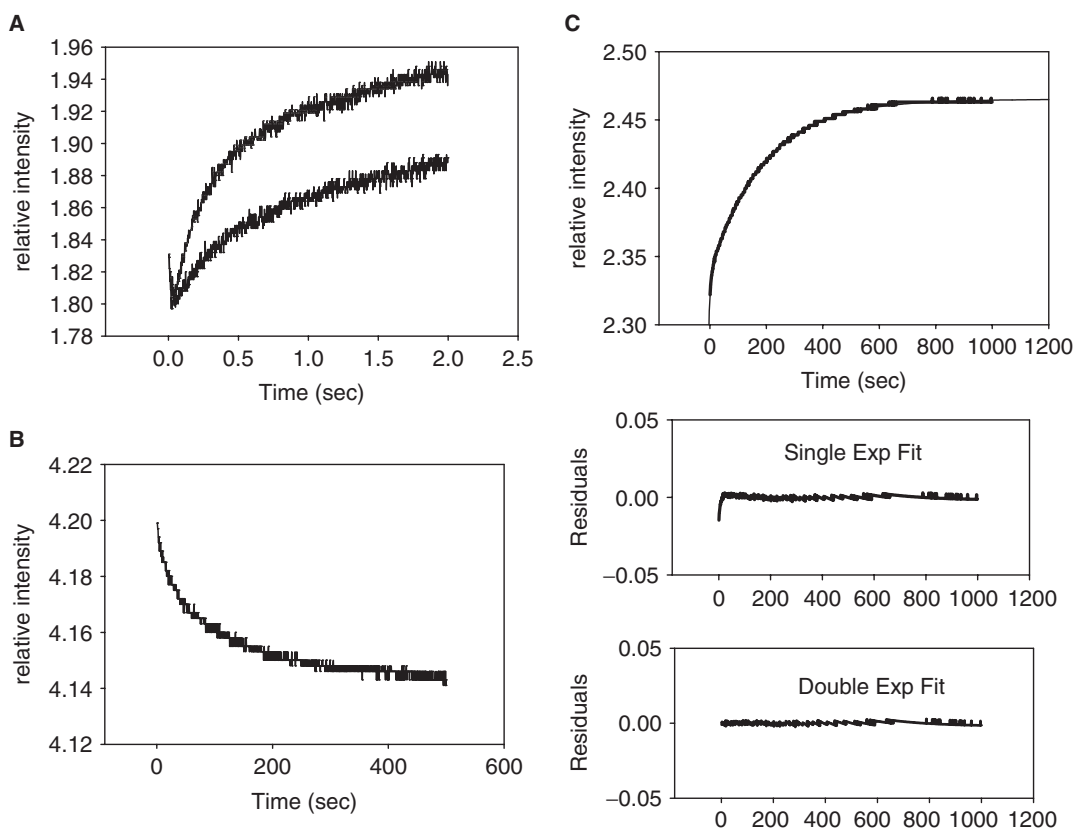
**Figure 3.** Stopped flow measurements of bending/intercalation and unbending/unintercalation for cognate DNA. (**A**) H235N M.EcoRI concentration-dependent forward bending at 4°C. Fluorescently labeled DNA (20 nM) was rapidly mixed with sinefungin (6 μM) and H235N M.EcoRI at two different concentrations (100 nM and 300 nM) to reveal rate dependence on concentration. Forward FRET experiments were done at 4°C to reveal the bending transition (initial decrease in donor emission). (**B**) WT M.EcoRI unbending and (**C**) H235N M.EcoRI unbending. A preformed complex of M.EcoRI (100 nM)-DNA (20 nM)-Sinefungin (6 μM) was rapidly mixed with 50-fold excess competitor DNA (5 μM), while the change in the donor fluorescence was monitored. H235N M.EcoRI unbending data fit best to a double exponential equation. Unbending/unintercalating rates were fit to a double exponential equation with residual analysis for single and double exponential fits below the corresponding plot.

conformations in which 2AP is efficiently quenched by charge transfer with neighboring bases, primarily electron transfer from guanine. The longest lifetime of 8.7 ns is due to 2AP in an unquenched extrahelical environment, only 6% ($A_4$) of the duplexes exist in this conformational state. Both WT and H235N M.EcoRI induce changes in the fluorescence decay parameters (Table 3) that are characteristic of base flipping: a marked decrease in the amplitudes of the shortest lifetime components (from 85% in total to 48%) and increase in amplitude of the longest lifetime (unquenched) component (from 6 to 53%) (9,10). The marked qualitative change in the 2AP fluorescence decay on base flipping is illustrated in Figure 5 which compares the decay curves of the cognate duplex unbound and when bound to the WT enzyme. The large increase in the average decay time (from 1.0 to 5.1 ns), that occurs when 2AP is transferred from the intrahelical (Figure 5A) to the extrahelical (Figure 5B) environment, is apparent.

Although the decays of the M.EcoRI–DNA complexes can be defined by four exponential terms, the number of conformational states present is likely to be much >4, given the intrinsic conformational heterogeneity of the duplex and the evidence from our previous studies of
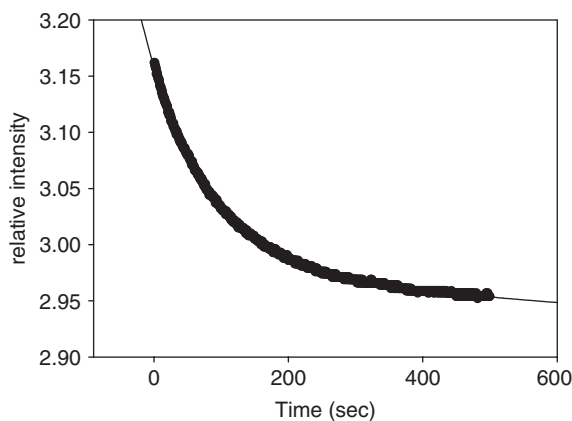
**Table 1.** WT and H235N M.EcoRI reverse bending/intercalating kinetics of cognate DNA

| Enzyme | Amp 1 (%) | Rate 1 ($s^{-1}$) | Amp 2 (%) | Rate 2 ($s^{-1}$) |
|---|---|---|---|---|
| WT M.EcoRI | 100 | 0.016 | – | – |
| H235N M.EcoRI | 13 | 0.17 | 87 | 0.0052 |

crystalline complexes of M.HhaI (9) and M.TaqI (10) that the base-flipped intermediate also exists in several conformational states. Each lifetime, therefore, represents a distribution of conformations in which 2AP experiences similar quenching rates. Thus for example, the 0.17 ns lifetime measured for CDM + WT M.EcoRI at equilibrium (Table 3) represents an average lifetime of 2AP in intrahelical (highly quenched) conformations of the unflipped intermediates E•DNA and E•DNA* (Scheme 1) and the fractional amplitude ($A_1$) of this lifetime component represents the total fractional population of such conformations in both intermediates. In a similar fashion, the 8.4 ns lifetime of CDM/WT M.EcoRI can be associated with conformations in which 2AP is

flipped out of the duplex in intermediates E∙DNA** and E∙DNA*** It follows, therefore, that differences in the populations of intermediates will be manifested as differences in the amplitudes and/or lifetime values measured in the fluorescence decay. Thus, the observation of shorter lifetimes for H235N M.EcoRI than for WT M.EcoRI (Table 3) are consistent with a different partitioning between intermediates for the mutant and WT enzymes, although the base-flipped (unquenched) intermediates are highly populated in both cases.

Combining information obtained from transient fluorescence of forward and reverse DNA bending, intercalation and base flipping (Figure 3 and Table 1), with equilibrium lifetime fluorescence of 2AP in DNA (Table 3) allows for a clear and encompassing, albeit indirect



**Figure 4.** Restacking kinetics for H235N M.EcoRI. Restacking rates were obtained by rapidly mixing a preformed complex of M.EcoRI (200 nM)-DNA (100 nM)-Sinefungin (6 µM) with 25-fold (5 µM) excess competitor DNA while monitoring the loss of 2AP fluorescence. H235N M.EcoRI restacking rates were fit to a double exponential equation similar to results previously published with WT M.EcoRI (23).

**Table 2.** WT and H235N M.EcoRI target base restacking kinetics of cognate DNA

| Enzyme | Amp 1 (%) | Rate 1 (s$^{-1}$) | Amp 2 (%) | Rate 2 (s$^{-1}$) |
|---|---|---|---|---|
| WT M.EcoRI | 38 | 0.089 | 62 | 0.022 |
| H235N M.EcoRI | 27 | 0.021 | 73 | 0.0054 |

**Table 3.** Fluorescence lifetimes ($\tau_i$) and their fractional amplitudes ($A_i$) for the 2AP-containing cognate duplex (CBM) alone and in the presence of WT and H235N M.EcoRI

| Solution composition | $\tau_1$ (ns) | $\tau_2$ (ns) | $\tau_3$ (ns) | $\tau_4$ (ns) | $A_1$ | $A_2$ | $A_3$ | $A_4$ | $\Phi_{rel}$ |
|---|---|---|---|---|---|---|---|---|---|
| CBM alone | 0.14 | 0.54 | 2.6 | 8.7 | 0.50 | 0.35 | 0.09 | 0.06 | 0.10 |
| CBM + WT M.EcoRI | 0.17 | 1.27 | 4.4 | 8.4 | 0.24 | 0.14 | 0.09 | 0.53 | 0.49 |
| CBM + H235N M.EcoRI | 0.16 | 0.88 | 3.9 | 8.0 | 0.25 | 0.13 | 0.08 | 0.54 | 0.46 |

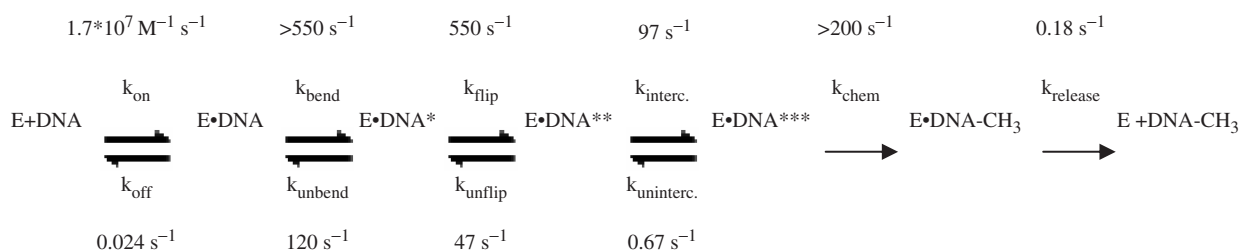The quantum yield relative to that of free 2AP riboside is also given.

comparison between WT and H235N M.EcoRI and their interactions with a target DNA. Such analysis reveals that of the three intermediates listed (bent DNA, flipped target base, intercalated DNA) the mutant enzyme, compared to the WT enzyme, at equilibrium has a 'fully flipped' target base (Table 3), yet the intercalation intermediate of the mutant enzyme is not as stable as the WT enzyme (Figure 3 and Table 1).

**Noncognate substrates favor a noncatalytic intermediate**

To better understand the enhanced substrate discrimination of H235N M.EcoRI, 2AP fluorescence decays with WT and H235N M.EcoRI bound to A4 noncognate DNA were collected. As illustrated in Figure 6, the decay curve of the noncognate duplex (Figure 6A) is virtually unchanged by binding to the mutant enzyme (Figure 6B), but is substantially lengthened by binding to the WT enzyme (Figure 6C). Comparison of the decay data in Tables 3 and 4 demonstrates a dramatic difference in the populations of enzyme-bound intermediates between cognate and noncognate substrates for both WT and H235N M.EcoRI. Binding of WT M.EcoRI with noncognate DNA (Table 4) results in a significant increase in population of conformations with extrahelical 2AP target base (increase in $A_4$ to 19% compared with 9% for the free duplex), although this is much less than observed with the cognate substrate. The qualitative difference in the decay curves is apparent in Figures 5 and 6. The decay of the noncognate duplex bound to WT M.EcoRI (Figure 6C) is significantly longer than that of the free duplex (Figure 6A) but much shorter than that of the cognate duplex bound to the WT enzyme (Figure 5B). Increases in $\tau_2$ and $\tau_3$ (relative to the free DNA) indicate the presence of conformations in which 2AP is quenched to a lesser extent than in the intrahelical environment. The population and lifetime of the shortest decay component ($A_1$ and $\tau_1$) appear to be unaffected in the presence of the enzyme, implying that the predominant conformation remains one in which 2AP is stacked in the duplex. This supports previous evidence that partitioning of the enzyme/DNA intermediates away from the catalytic
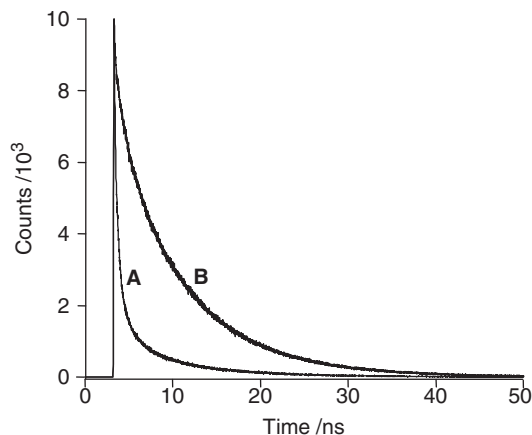


**Figure 5.** The fluorescence decay curve of (**A**) the 2AP-containing cognate duplex alone and (**B**) the 2AP-containing cognate duplex complexed with WT M.EcoRI and sinefungin.

$$1.7*10^7\ M^{-1}\ s^{-1} \qquad >550\ s^{-1} \qquad 550\ s^{-1} \qquad 97\ s^{-1} \qquad >200\ s^{-1} \qquad 0.18\ s^{-1}$$

$$\text{E+DNA} \underset{k_{off}}{\overset{k_{on}}{\rightleftharpoons}} \text{E}\cdot\text{DNA} \underset{k_{unbend}}{\overset{k_{bend}}{\rightleftharpoons}} \text{E}\cdot\text{DNA}^* \underset{k_{unflip}}{\overset{k_{flip}}{\rightleftharpoons}} \text{E}\cdot\text{DNA}^{**} \underset{k_{uninterc.}}{\overset{k_{interc.}}{\rightleftharpoons}} \text{E}\cdot\text{DNA}^{***} \overset{k_{chem}}{\longrightarrow} \text{E}\cdot\text{DNA-CH}_3 \overset{k_{release}}{\longrightarrow} \text{E +DNA-CH}_3$$

$$0.024\ s^{-1} \qquad\qquad 120\ s^{-1} \qquad\qquad 47\ s^{-1} \qquad\qquad 0.67\ s^{-1}$$

**Scheme 1.** Kinetic mechanism of M.EcoRI. E▪DNA indicates an unbent enzyme–DNA complex. E▪DNA* indicates a bent enzyme–DNA complex. E▪DNA** indicates a base-flipped complex. E▪DNA*** indicates an intercalated complex. DNA-CH3 is the N6 methylated DNA. Bending and intercalation are monitored with FRET. Flipping is monitored with 2-aminopurine fluorescence. The chemistry step is measured by single turn-over experiments. Rate constants for individual steps in the reaction mechanism are listed above the corresponding step. Values for $k_{on}$, $k_{off}$, $k_{chem}$ and product release were obtained from Allan *et al.* (23). Values for $k_{bend}$ $k_{flip}$ and $k_{interc.}$ were obtained from Youngblood and Reich (12). It should be noted that the values from Youngblood *et al.* were determined using a global fitting analysis of data obtained at 4°C.
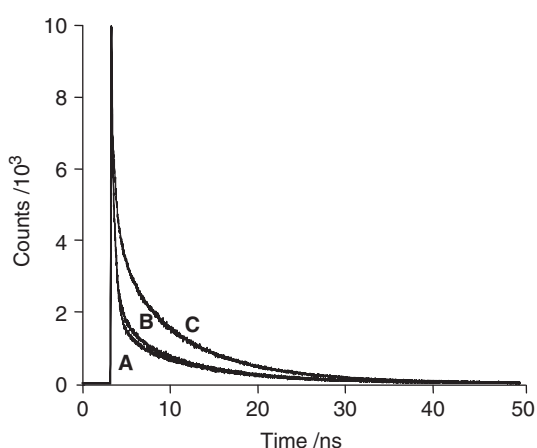


**Figure 6.** The fluorescence decay curve of (**A**) the 2AP-containing noncognate duplex alone, (**B**) the 2AP-containing noncognate duplex complexed with H235N M.EcoRI and sinefungin and (**C**) the 2AP-containing noncognate duplex complexed with WT M.EcoRI and sinefungin.

**Table 4.** Fluorescence lifetimes ($\tau_i$) and their fractional amplitudes ($A_i$) for the 2AP-containing noncognate duplex (A4) alone and in the presence of WT and H235N M.EcoRI

| Solution composition | $\tau_1$ (ns) | $\tau_2$ (ns) | $\tau_3$ (ns) | $\tau_4$ (ns) | $A_1$ | $A_2$ | $A_3$ | $A_4$ | $\Phi_{rel}$ |
|---|---|---|---|---|---|---|---|---|---|
| A4 alone | 0.15 | 0.46 | 2.5 | 9.9 | 0.51 | 0.36 | 0.04 | 0.09 | 0.12 |
| A4 + WT M.EcoRI | 0.17 | 0.74 | 3.6 | 9.2 | 0.49 | 0.23 | 0.09 | 0.19 | 0.25 |
| A4 + H235N M.EcoRI | 0.15 | 0.49 | 2.7 | 9.6 | 0.51 | 0.33 | 0.07 | 0.10 | 0.13 |

The quantum yield relative to that of free 2AP riboside is also given.

complex and toward the unbent intermediate is favored with noncognate substrates (12).

For the noncognate substrate with H235N M.EcoRI, all of the decay parameters are essentially unchanged compared with the free duplex; the two decay curves are almost identical, as shown in Figure 6. This indicates that the equilibrium population is heavily biased toward unflipped intermediates in which the environment of

2AP is largely unaffected by the presence of the enzyme. It follows that the quantum yield for 2AP in the non-cognate substrate A4 should not change when bound by H235N M.EcoRI ($\Phi_{rel}$ in Table 4). This explains why we observe no change in transient (measured with a stopped-flow apparatus) or equilibrium fluorescence intensity when monitoring 2AP containing A4 noncognate DNA with H235N M.EcoRI (data not shown).

## DISCUSSION

The challenge faced by enzymes that sequence-specifically modify DNA provides an excellent opportunity to investigate the basis of enzyme specificity. DNA methyltransferase discrimination is partly accomplished by exploiting large-scale conformational changes both within the enzyme and the target DNA. Conformational changes in the DNA substrate have been previously characterized with the DNA adenine methyltransferase M.EcoRI (12,13,16–18). The M.EcoRI-induced changes in DNA conformation, including bending, flipping and intercalation provide a compelling basis for regulating sequence discrimination (12). Early evidence for this was provided by a bending-impaired H235N M.EcoRI whose decreased apparent base-flipping constant also resulted, paradoxically, in a dramatic increase in the mutant's ability to recognize its target sequence (13).

The searching mechanism of DNA-modifying enzymes often involves a random one-dimensional search or 'facilitated diffusion' along the genomic DNA in addition to three-dimensional diffusion (24). When bound to the DNA, enzymes have evolved a way to select against noncognate substrates that does not dramatically affect the affinity for the DNA; a weakened affinity would lead to frequent loss of contact with the DNA molecule. In the case of M.EcoRI, the affinity for noncognate and cognate substrates is similar which is consistent with the use of facilitated diffusion mechanism by M.EcoRI (12,19,20,23). Interestingly, WT M.EcoRI has a 2500-fold difference in methylation specificity between site A4 and cognate DNA, yet there is only ~7-fold change in affinity between the two sites (11). We recently reported that the partitioning between conformational intermediates away from the chemistry step provides some of the

specificity of M.EcoRI (12). Thus, by differentially over-populating an intermediate that does not allow chemistry to occur but still allows the enzyme to stay bound to the substrate, facilitated diffusion is possible.

The work presented here reveals that indeed the H235N mutation causes a redistribution of conformational intermediates accounting for the enhanced specificity for its cognate sequence. It was previously believed that the H235N mutation resulted in a bending-deficient enzyme (13). Our transient FRET experiments reveal that in fact a bending phase is still observed with H235N M.EcoRI, and that the intercalation step is impacted (Figure 3A and C). A plausible explanation of this bending-impaired mutant is provided by the transient fluorescence results. If a step in the reaction mechanism following bending is destabilized, then the enzyme–DNA complex will favor earlier intermediates in the reaction, namely the bent and unbent states as is apparent by examining the numerical contributions to each intermediate. (Scheme 1); $[E \cdot DNA] = k_{on}[E] - k_{off}[E \cdot DNA] - k_{bend}[E \cdot DNA] + k_{unbend}[E \cdot DNA^*]$. Since $k_{unbend}$ $[E \cdot DNA^*]$ positively contributes to increases in $[E \cdot DNA]$, as $[E \cdot DNA^*]$ concentration increases, the concentration of $[E \cdot DNA]$ will also follow this trend. Thus, when the bend angles for a large sampled population of H235N M.EcoRI–DNA complexes are observed by AFM it appears as if there is little bent DNA as there is more unbent DNA than with the wild-type M.EcoRI. Our FRET results with cognate DNA support this interpretation as it appears as if there is relatively little H235N M.EcoRI-induced conformational change to the cognate DNA (Figure 2).

The temporal relationship between the mechanistic steps of DNA bending, base flipping and intercalation is shown in Scheme 1 (12,16,23). Although all steps occur very rapidly, the intercalation step follows base flipping. Since the mutant H235N M.EcoRI appears to be impaired in its ability to stabilize an intercalated intermediate with cognate DNA it seems reasonable that the stabilization of the flipped target base may also be reduced. However, the destabilization of the flipped state is relatively small with cognate DNA. We observe that the restacking rate constant, $k_{unflip}$, of H235N M.EcoRI is only ∼4-fold slower with cognate DNA (Table 2, Figure 4) and the fluorescence decay data for cognate DNA containing 2AP (Table 3) are similar for both enzymes. The slightly shorter lifetimes for H235N M.EcoRI suggest that the inability to retain an intercalated/flipped DNA intermediate results in a more quenched environment for the target base.

A clear distinction in the populated intermediates is observable when WT and H235N M.EcoRI are bound to noncognate substrate A4 (Table 4). When WT M.EcoRI binds, there is a significant population of intermediates in which 2AP is extrahelical, although intermediates in which 2AP remains intrahelical dominate. For H235N EcoRI, the population is shifted so far toward unflipped intermediates that the decay parameters show no evidence of base flipping, or indeed any perturbation of the 2AP environment. Thus, a measurable difference in the catalytic complex should be observable comparing WT and H235N M.EcoRI with noncognate DNA. As can be

**Table 5.** Michaelis constants of M.EcoRI for cognate and noncognate substrates

| Enzyme | CBM (nM) | A4 (nM) | A4 (nM)[a] |
|---|---|---|---|
| WT M.EcoRI | $80 \pm 26$ | $1900 \pm 590$ | $330 \pm 75$ |
| H235N M.EcoRI | $55 \pm 8.7$ | $3800 \pm 720$ | $800 \pm 130$ |

[a]Star conditions performed with 32-mer substrate to replicate previous specificity enhancement observation (13).

seen in Table 5, the Michaelis constant for cognate DNA is similar for both enzymes but if one compares the $K_M$ for cognate versus noncognate for each enzyme, then it is apparent that the mutant has a better ability to reach the Michaelis complex than the WT enzyme. Our data indicate that this is because the mutant enzyme does not waste time attempting to flip out a base in a noncognate sequence whereas the wild-type enzyme does perform some flipping on a noncognate sequence. Interestingly, we do not observe a difference in specificity ($k_{cat}/K_M$) between the mutant and WT enzyme with this noncognate substrate. The previous characterization of specificity enhancement for H235N M.EcoRI was performed with plasmid DNA as a substrate (13). Our lack of observing any change in specificity may be due to the size of the substrate, which is necessary for our biochemical analysis. Our prior characterization of M.EcoRI kinetic proofreading is further complemented by the analysis presented here of the specificity-enhanced H235N M.EcoRI. Kinetic proofreading used by M.EcoRI allows for the efficient selection of the cognate site over the noncognate sites and involves conformational checkpoints which contribute to the specificity of the enzyme. Examination of changes to the local environment, which perturb the conformational intermediates, has provided more insight into DNA methyltransferase proofreading. Here we have confirmed, using the added resolution of time-resolved fluorescence, that DNA-modifying enzymes may be engineered to selectively alter the conformational partitioning between different substrates.

## ACKNOWLEDGEMENT

## REFERENCES

1. Jeltsch,A. (2002) Beyond Watson and Crick: DNA methylation and molecular enzymology of DNA methyltransferases. *Chembiochem*, **3**, 274–293.
2. Heithoff,D.M., Sinsheimer,R.L., Low,D.A. and Mahan,M.J. (1999) An essential role for DNA adenine methylation in bacterial virulence. *Science*, **284**, 967–970.
3. Jones,P.A. (2003) Epigenetics in carcinogenesis and cancer prevention. *Ann. NY Acad. Sci.*, **983**, 213–219.
4. Mashhoon,N., Carroll,M., Pruss,C., Eberhard,J., Ishikawa,S., Estabrook,R.A. and Reich,N. (2004) Functional characterization of Escherichia coli DNA adenine methyltransferase, a novel target for antibiotics. *J. Biol. Chem.*, **279**, 52075–52081.

5. Robertson,K.D. and Wolffe,A.P. (2000) DNA methylation in health and disease. *Nat. Rev. Genet.*, **1**, 11–19.
6. Klimasauskas,S., Kumar,S., Roberts,R.J. and Cheng,X. (1994) HhaI methyltransferase flips its target base out of the DNA helix. *Cell*, **76**, 357–369.
7. Cheng,X. and Roberts,R.J. (2001) AdoMet-dependent methylation, DNA methyltransferases and base flipping. *Nucleic Acids Res.*, **29**, 3784–3795.
8. Allan,B.W. and Reich,N.O. (1996) Targeted base stacking disruption by the EcoRI DNA methyltransferase. *Biochemistry*, **35**, 14757–14762.
9. Neely,R.K., Daujotyte,D., Grazulis,S., Magennis,S.W., Dryden,D.T., Klimasauskas,S. and Jones,A.C. (2005) Time-resolved fluorescence of 2-aminopurine as a probe of base flipping in M.HhaI-DNA complexes. *Nucleic Acids Res.*, **33**, 6953–6960.
10. Lenz,T., Bonnist,E.Y., Pljevaljcic,G., Neely,R.K., Dryden,D.T., Scheidig,A.J., Jones,A.C. and Weinhold,E. (2007) 2-Aminopurine flipped into the active site of the adenine-specific DNA methyltransferase M.TaqI: crystal structures and time-resolved fluorescence. *J. Am. Chem. Soc.*, **129**, 6240–6248.
11. Reich,N.O., Olsen,C., Osti,F. and Murphy,J. (1992) In vitro specificity of EcoRI DNA methyltransferase. *J. Biol. Chem.*, **267**, 15802–15807.
12. Youngblood,B. and Reich,N.O. (2006) Conformational transitions as determinants of specificity for the DNA methyltransferase EcoRI. *J. Biol. Chem.*, **281**, 26821–26831.
13. Allan,B.W., Garcia,R., Maegley,K., Mort,J., Wong,D., Lindstrom,W., Beechem,J.M. and Reich,N.O. (1999) DNA bending by EcoRI DNA methyltransferase accelerates base flipping but compromises specificity. *J. Biol. Chem.*, **274**, 19269–19275.
14. Donlin,M.J., Patel,S.S. and Johnson,K.A. (1991) Kinetic partitioning between the exonuclease and polymerase sites in DNA error correction. *Biochemistry*, **30**, 538–546.
15. Johnson,K A. (1993) Conformational coupling in DNA polymerase fidelity. *Annu. Rev. Biochem.*, **62**, 685–713.
16. Hopkins,B.B. and Reich,N.O. (2004) Simultaneous DNA binding, bending, and base flipping: evidence for a novel M.EcoRI methyltransferase-DNA complex. *J. Biol. Chem.*, **279**, 37049–37060.
17. Allan,B.W., Beechem,J.M., Lindstrom,W.M. and Reich,N.O. (1998) Direct real time observation of base flipping by the EcoRI DNA methyltransferase. *J. Biol. Chem.*, **273**, 2368–2373.
18. Su,T.J., Tock,M.R., Egelhaaf,S.U., Poon,W.C. and Dryden,D.T. (2005) DNA bending by M.EcoKI methyltransferase is coupled to nucleotide flipping. *Nucleic Acids Res.*, **33**, 3235–3244.
19. Rachofsky,E.L., Seibert,E., Stivers,J.T., Osman,R. and Ross,J.B. (2001) Conformation and dynamics of abasic sites in DNA investigated by time-resolved fluorescence of 2-aminopurine. *Biochemistry*, **40**, 957–967.
20. Estabrook,R.A., Lipson,R., Hopkins,B. and Reich,N. (2004) The coupling of tight DNA binding and base flipping: identification of a conserved structural motif in base flipping enzymes. *J. Biol. Chem.*, **279**, 31419–31428.
21. Sharma,V., Youngblood,B. and Reich,N. (2005) Residues distal from the active site that alter enzyme function in M.HhaI DNA cytosine methyltransferase. *J. Biomol. Struct. Dyn.*, **22**, 533–544.
22. Lindstrom,W.M.,Jr, Flynn,J. and Reich,N. O. (2000) Reconciling structure and function in HhaI DNA cytosine-C-5 methyltransferase. *J. Biol. Chem.*, **275**, 4912–4919.
23. Allan,B.W., Reich,N.O. and Beechem,J.M. (1999) Measurement of the absolute temporal coupling between DNA binding and base flipping. *Biochemistry*, **38**, 5308–5314.
24. Halford,S.E. and Marko,J.F. (2004) How do site-specific DNA-binding proteins find their targets? *Nucleic Acids Res.*, **32**, 3040–3052.